Timo Dobler[1,*,‡]
Stefan Höving[2,*,‡]
Christian Dreiser[3]
Marco Gleiß[1]
Mathias Gröschen[3]
Alexander Henkel[4]
Manuel Hörne[5]
Martin Schäfer[4]
Jana Sonnenschein[6]
Georg Wiese[7]
Kerstin Wohlgemuth[6]
Norbert Kockmann[2]
Hermann Nirschl[1]

From Lab to Pilot Scale: Commissioning of an Integrated Device for the Generation of Crystals

Fast time-to-market, increased efficiency, and flexibility of production processes are major motivators for the development of integrated, continuous apparatuses with short changeover times. Following this trend, the modular belt crystallizer was developed and characterized in lab scale with the model system sucrose-water. Based on the promising results, the plant concept was upscaled and commissioned in industrial environment. The results are presented within the scope of this work. Starting from small seed crystals in solution, it was possible to grow, separate, and dry product particles. Further, the conducted experiments demonstrated that it is feasible to transfer the results from laboratory to pilot scale, which in turn enables accelerated process design as well as development.

Keywords: Batch-to-continuous production, Crystal generation, Integrated process design, Modularization, Plant commissioning

Received: December 22, 2022; *accepted:* March 31, 2023

DOI: 10.1002/ceat.202200616

1 Introduction

Increasing competition, volatile markets, and rising energy prices are some of the most important innovation drivers in the chemical industry [1, 2]. To meet and tackle these challenges successfully, innovative solutions are needed. That includes, for example, the establishment of continuous processes and the development of flexible, modular, and integrated plant concepts [3].

In the field of pharmaceutical and specialty chemicals in particular, there is a trend toward continuous processes. Compared with conventional batch operation, the energy required for start-up and shut-down procedures is significantly reduced [4, 5]. In addition, continuous processes offer shorter idle and cleaning times, higher production capacities, and constant product quality [1, 4]. Since solids handling is often an essential part of fine chemical processes, continuous operation is necessary for crystallization, too. Considering this, there has been a consistent paradigm shift in the field of crystallization in the recent years, which in turn is demonstrated by the development of numerous new continuous plant concepts [6–10].

Apart from the mode of operation, the modularization of apparatuses is also gaining relevance. The use of standardized modular components that are applicable for multiple processes ensures a shortened time-to-market and enables straightforward adaptation to changing customer requirements [3, 11]. This includes both minor changes within existing manufacturing routes as well as the quick and easy realization of complete product changes. Another advantage of modular systems is the comparatively low investment costs, which arise from the recycling of existing modules and the reduced design effort [3, 11]. Numerous modular equipment concepts have already been described in the literature. An example is a miniplant for the production and separation of amino acids described in

[1]Timo Dobler https://orcid.org/0000-0002-3817-6058 (timo.dobler@kit.edu), Marco Gleiß, Prof. Hermann Nirschl
Karlsruhe Institute of Technology, Institute of Mechanical Process Engineering and Mechanics, Strasse am Forum 8, 76131 Karlsruhe, Germany.

[2]Stefan Höving https://orcid.org/0000-0002-9083-3318 (stefan.hoeving@tu-dortmund.de), Prof. Norbert Kockmann https://orcid.org/0000-0002-8852-3812
TU Dortmund University, Laboratory of Equipment Design, Emil-Figge-Strasse 68, 44227 Dortmund, Germany.

[3]Dr. Christian Dreiser, Mathias Gröschen
Clariant Produkte (Deutschland) GmbH, Brünningstrasse 50, 65929 Frankfurt, Germany.

[4]Alexander Henkel, Martin Schäfer
BHS-Sonthofen GmbH, An der Eisenschmelze 47, 87527 Sonthofen, Germany.

[5]Manuel Hörne
HiTec Zang GmbH, Ebertstrasse 28–32, 52134 Herzogenrath, Germany.

[6]Jana Sonnenschein, Dr. Kerstin Wohlgemuth https://orcid.org/0000-0001-7914-4303
TU Dortmund University, Laboratory of Plant and Process Design, Emil-Figge-Strasse 70, 44227 Dortmund, Germany.

[7]Georg Wiese
SONOTEC GmbH, Neuendorfer Strasse 2, 06112 Halle, Germany.

[‡]Both authors contributed equally to this paper.

Hohmann et al. [12]. A proof-of-concept was achieved by experiments with the substance system L-alanine [12]. Another example is the vacuum screw filter, which was developed by Steenweg et al. and allows the combined washing and dehumidification of previously manufactured L-alanine crystals [13, 14].

Furthermore, the integration of several process steps in a single apparatus is attracting more and more research attention. The main advantages are the minimized risk of contamination, the small space requirement, and the elimination of transport equipment [15]. On the one hand, this improves product quality and, on the other hand, reduces acquisition costs. Examples from the field of process engineering are the Titus-Nutschen Dryer [16] and the belt crystallizer first discussed in Dobler et al. [15]. The latter is a modified belt filter that incorporates the unit operations crystallization, solid-liquid separation, washing, and drying. The functionality of the device was demonstrated by experiments with sucrose-water [15].

In a consecutive study, Dobler et al. [17] demonstrated that the concept is also suitable for the production and separation of rod-shaped and isometric lysozyme crystals using evaporation crystallization into vacuum. Further investigations by Höving et al. [18] found that Peltier elements allow for precise temperature control of the crystal suspension during the crystallization and that the seed particles and temperature management exert a significant influence on the resulting product crystals. Parallel to experimental investigations, a model for the integrated apparatus was set up by Sonnenschein et al. [19] to reduce experimental effort when switching substance systems.

So far, all experiments using the belt crystallizer have been carried out on laboratory scale [5, 15, 18]. Based on the promising results generated in this way, a scale-up to pilot level seems reasonable. However, this is not trivial and only rarely described in detail in the literature [12]. Therefore, the following publication investigates the possibility of transferring the results from laboratory to industrial scale. For this purpose, a pilot plant is put into operation. Subsequently, the results obtained are compared with those from the laboratory scale and differences are discussed.

2 Materials and Methods

In the following section, the apparatus concept, the particle system, the numerical model approach as well as the experimental procedure and the evaluation are discussed.

2.1 Pilot Plant

The pilot plant used in this work is based on the laboratory-scale belt crystallizer [5, 15, 18] and includes the process steps crystallization, solid-liquid separation, washing, and drying. The setup is schematically displayed in Fig. 1. The apparatus concept is described in detail in Löbnitz [5], Dobler et al. [15], and Höving et al. [18].

Analogous to the belt crystallizer, the basis of the applied device is a belt filter, in which the vacuum trays below the filter medium are replaced by flexible and arbitrarily combinable functional units. In the region of crystallization and drying, temperature segments are used. For solid-liquid separation, filtration elements are located below the filter medium. The particle production and separation process itself takes place above the filter medium in detached zones. These zones pass incrementally through the process chain from left to right, where a crystal growth is induced by cooling, starting from an inoculated seed suspension. Subsequently, the solid and liquid components are separated by an applied pressure difference. Finally, the remaining wet particles get thermally dried and the valuable product is removed from the filter. Any impurities still existing on the filter medium are eliminated by high-pressure nozzles. In contrast to the belt crystallizer in [15] and [18], the individual zones are not separated by process chambers placed on top of the filter, but by separator plates that are moving with the filter belt. The movement of these separator plates is synchronized with the cycle time t_{cycle} of the filter, which in turn enables precise positioning of the zones directly above the individual functional units.

In Fig. 2, an image of the pilot plant constructed by BHS-Sonthofen GmbH (Sonthofen, Germany) and automated by HiTec Zang GmbH (Herzogenrath, Germany) is given. Including the housing, it measures about 2.20 m in height, 2 m in width, and 1 m in depth and offers space for up to ten interchangeable functional units below the filter medium (dimensions do not include the feed storage and preparation). Since all of these units have identical dimensions of 0.1 m×0.1 m, it is possible to configure the plant to customer specifications.

The entire system can be divided into five sections (100–500). For a better understanding of their structure and technical realization, the piping and instrumentation diagram can be found in Fig. A1 in the Appendix.

– *100: Feed Preparation.* This section includes all components required to prepare and feed the seed suspension onto the apparatus. It comprises a thermostat (TH105), a double-walled tank with agitator (B101), temperature and pH sensors, and a dosing pump (P106). The latter is used to add

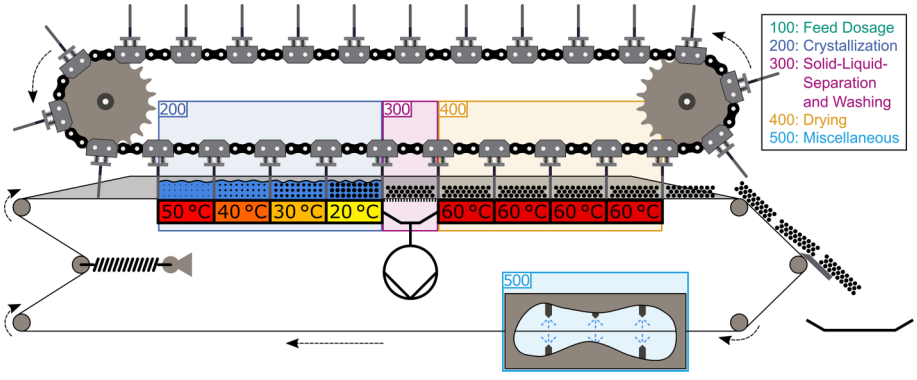

Figure 1. Schematic illustration of the pilot plant. The process medium separated by the separator plates move from left to right.

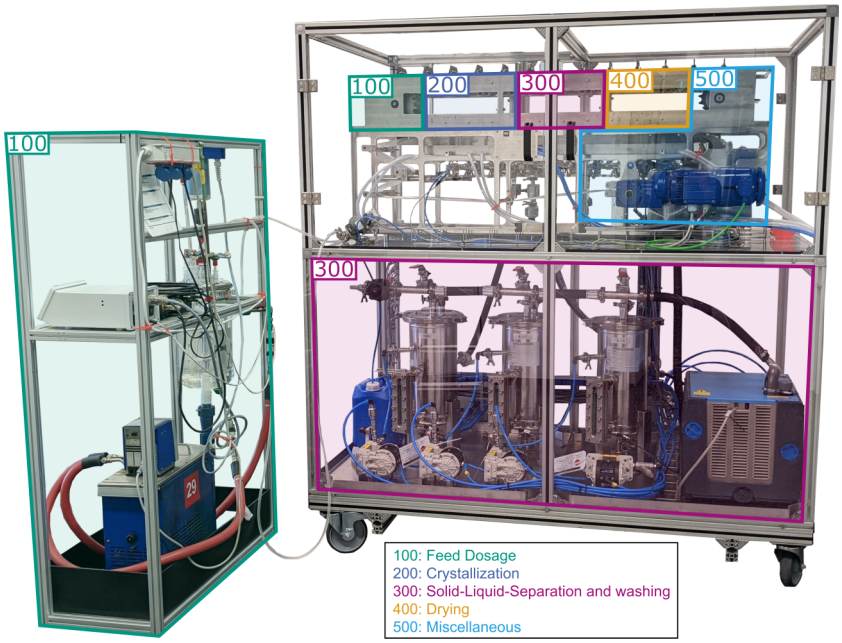

Figure 2. Photograph of the pilot plant. Area 100 is used to prepare the feed suspension and add it to the filter. In zones 200, 300, and 400, the manufacturing and separation process takes place. The length of the zones depends on the number of functional units used in the individual areas. Section 500 comprises all other components of the pilot plant. These include the motors and cleaning nozzles.

the preheated suspension to the filter via a feed unit. To prevent crystallization of the sample within the tubes and pipelines, it is constantly pumped in the circuit. Feeding is achieved by opening a pressure relief valve (V108). The feed volume may be set individually and is monitored and controlled by means of an inline sensor (SONOTEC GmbH, Halle, Germany).

- *200: Crystallization.* In this area, particle growth take place. Therefore, temperature units (FU204-207) are installed below the filter medium. Every single unit consists of a square stainless-steel plate (0.1 m×0.1 m), which contains channels for cooling or heating liquid. The channels are arranged in such a way that a homogeneous plate temperature is achieved. The temperature is adjusted by a thermostat (TH201-203) or by connection to a cooling or heating circuit. It is possible to actuate each functional unit individually, so that any temperature profile becomes feasible (here: 50 °C – 40 °C – 30 °C – 20 °C). As a consequence, the apparatus concept is also suitable for other types of crystallization than cooling crystallization, e.g., precipitation with subsequent aging at constant temperature. For process monitoring and control, the individual units are equipped with temperature sensors.
- *300: Solid-liquid separation and cake washing.* To separate the solid and liquid components, filtration units (FU305-309) are deployed. These are stainless-steel plates (0.1 m×0.1 m) with small holes (d = 3 mm) on top. The bottom side of each assembly is provided with a connection to a vacuum pump (P334) and a valve (V305-309). To remove impurities and remaining mother liquor, the pilot plant also has two washing units, with nozzles that can provide a desired washing liquid, located above the filter cake. The filtrate produced during the separation and washing process is collected in three different tanks (B312, B319, and B326). This ensures that both the mother liquor and the washing liquids can be reused or recycled.
- *400: Drying.* In the drying zone, contact drying serves to reduce the moisture of the solid remaining on the filter medium. For this purpose, temperature units (FU402) are necessary. The design and mode of operation is analogous to the functional units located in the crystallization zone.
- *500: Miscellaneous.* This section deals with all other components of the pilot plant. It includes the motors for the filter (M501) and separator plates (M505), the balance for weighing the accumulated product (A502), and the cloth washing chamber. The latter removes any residues and impurities from the filter cloth by means of high-pressure nozzles. The respective cleaning time is variable and adjustable via valve (V504).

2.2 Model Substance System

The material system used to characterize the plant is a mixture of sucrose (Südzucker AG, Mannheim, Germany) and deionized water as solvent (< 10 µS cm^{-1}). In previous work, the lab-scale apparatuses in [15] and [18] has been operated and characterized with the respective system. Saturated solutions were prepared according to the correlation from Vavrinecz [20]:

$$w^* = 64.47 + 8.222\times10^{-2}T + 1.6169\times10^{-2}T^2 - 1.558\times10^{-6}T^3 - 4.63\times10^{-8}T^4 \quad (1)$$

Herein, w^*[1)] represents the solid mass fraction and T the temperature in °C. For the conducted experiments, the inoculated seed suspension was cooled down along the crystallization modules. For calculations regarding yield and excess crystal mass, the final temperature of the suspension was assumed to be 20 °C, which corresponds to the temperature of the final crystallization module.

All experiments involved an unstirred sucrose suspension with a height of 20 mm. The temperature profiles occurring within this suspension were modeled by Sonnenschein et al. [19] and can be seen in Fig. 3. The simulative observation at different positions (5, 10, and 15 mm above the functional unit) showed that there was a slight temperature gradient in the pro-

1) List of symbols at the end of the paper.

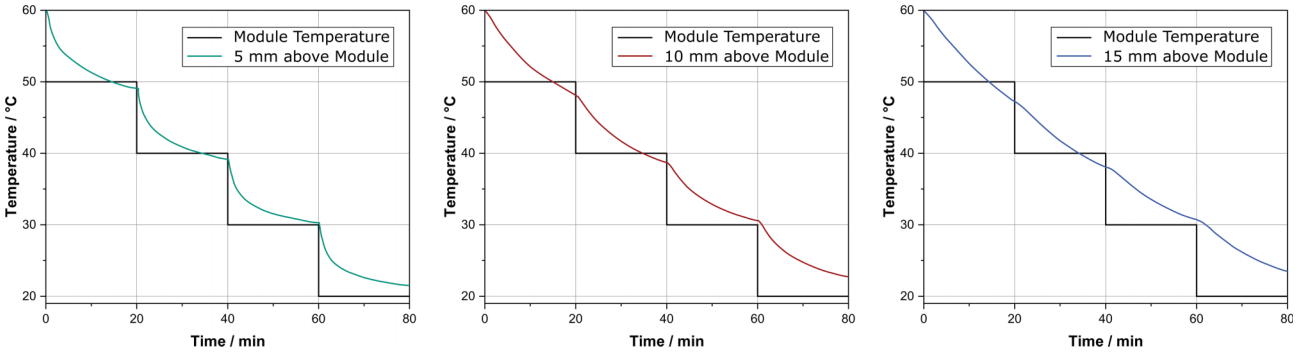

Figure 3. Simulated temperature profile of an unstirred sucrose suspension as a function of distance from the temperature unit. Adapted from [19].

cess medium depending on the distance to the temperature element. The authors' assumptions for the temperature settings and residence times at each module are consistent with the experiments performed in this work.

2.3 Modeling

The approach for modeling the cooling crystallization is based on a spatially resolved population balance equation coupled with solute mass and solute heat balances. A detailed description is given in Sonnenschein et al. [19].

Basis for the calculation of the solid-liquid separation was Darcy's law [21]. Using this formula, the filtrate volume occurring over time was estimated and the solvent content was determined according to Eq. (6). The porosity of the filter cake required for the computation of the cake height was approximated by an empirical approach of Tsotas [22]. To keep the computational effort as low as possible, liquid losses due to leakage or evaporation effects were neglected and complete removal of supersaturation during crystallization was assumed.

2.4 Experimental Procedure

The experiments were prepared by setting up sucrose solution (saturated at 60 °C) in a temperature-controlled flask (Schott AG, Mainz, Germany). For the dissolution of the solid component, the temperature was set to 65 °C, while shortly before the experiments it was lowered to 59 °C to reach a slight supersaturation and counteract the dissolution of seed crystals. Solutions were freshly prepared every day. Seed crystals were obtained from dry pestled and sieved sucrose particles. The resulting size distribution can be found in Fig. 5. For each experiment, 240 mL of saturated solution was thoroughly mixed with 1.83 g of seed crystals, which corresponds to 2.5 % excess crystal mass (ECM). The ECM is calculated as:

$$\mathrm{ECM} = \left(X_{\mathrm{theo},T_{\mathrm{start}}} - X_{\mathrm{theo},T_{\mathrm{end}}}\right) m_{\mathrm{ml}} x_{\mathrm{aq}} \tag{2}$$

where m_{ml} stands for the absolute mass of mother liquor, $X_{\mathrm{theo},T_{\mathrm{start}}}$ is the initial loading, $X_{\mathrm{theo},T_{\mathrm{end}}}$ is the theoretical final loading in thermodynamic equilibrium, and x_{aq} denotes the water content. The theoretical loading X_{theo,T_i} depends on the solids mass fraction and the temperature. The following applies:

$$X_{\mathrm{theo},T_i} = \frac{w_{T_i}^{\star}}{1 - w_{T_i}^{\star}} \tag{3}$$

During the entire course of the experiments, samples were taken from the suspension and the filter cake to determine the relative yield *Y*, the particle size distribution PSD, and the residual solvent content *SC*. Sampling was done every t_{cycle} right before the filter belt with process medium moves to the subsequent position. The filter medium used in all tests was an industrial cloth with a mesh size of 22 µm (Sefar AG, Heiden, Switzerland). The properties were similar to those of the filter medium investigated in Dobler et al. [15]. For this reason, it can be assumed that no blocking of the pores took place due to the crystallization process. A summary of the experimental conditions is given in Tab. 1.

Table 1. Operation parameters.

Parameter	Symbol	Value
Cycle time	t_{cycle} [min]	20
Sampling time	t_{sample} [min]	20
Saturation temperature	T_{sat} [°C]	60
Suspension temperature at start	T_{start} [°C]	59
Solution volume	V_{tot} [mL]	24
Seed crystal mass	m_{seed} [g]	1.83
Liquid level	h_{susp} [mm]	20
Number crystallization units	n_{cry} [–]	4
Crystallization module temperatures	T_{mod} [°C]	50 – 40 – 30 – 20
Number filtration units	n_{filt} [–]	1
Filtration pressure difference	Δp [mbar]	500
Number drying units	n_{dry} [–]	4
Drying temperature	T_{dry} [°C]	60

2.5 Analytics

2.5.1 Yield

To determine the yield and the process progress in relation to the thermodynamics, samples along the crystallization were taken using a 5-mL syringe (B. Braun SE, Melsungen, Germany). Afterwards, they were filtered with a reusable polycarbonate syringe filter holder equipped with a 1-µm pore size filter membrane (Pall GmbH, Dreieich, Germany). The clear mother liquor was then weighed (Kern & Sohn GmbH, Balingen, Germany) and placed in a vacuum oven at 600 mbar and 60 °C for two weeks to calculate the sucrose loading X.

$$X = \frac{m_{\mathrm{suc}}}{m_{\mathrm{water}}} \tag{4}$$

To get the relative yield Y of each sampling time, the following correlation was used:

$$Y = \frac{X_{\mathrm{theo},T_{\mathrm{sat}}} - X}{X_{\mathrm{theo},T_{\mathrm{sat}}} - X_{\mathrm{theo},T_{\mathrm{end}}}} \tag{5}$$

Herein, $X_{\mathrm{theo},T_{\mathrm{sat}}}$ is the loading of the saturated solution at the beginning and $X_{\mathrm{theo},T_{\mathrm{end}}}$ the theoretical loading of the solution in equilibrium at the end of the experiment.

2.5.2 Particle Size Distribution

For the measurement of the PSD, samples taken with a syringe (during crystallization) or a scoop (during solid-liquid separation) were analyzed with sedimentation analysis using an analytical photocentrifuge (LUM GmbH, Berlin, Germany). This instrument measures the temporal light transmission values at a wavelength of 865 nm and converts them into extinction profiles, which in turn are used to calculate the PSD. A detailed description of the device is given in Detloff et al. [23]. To achieve a suitable particle concentration and avoid bulk sedimentation, the samples were diluted to a solid concentration of 1 %. Therefore, saturated sucrose solution with the temperature of the respecting module was added to the sample. The centrifuge speed applied in all experiments was 1000 rpm [15].

2.5.3 Solvent Content

To characterize the solid-liquid separation and drying process, the remaining solvent content of the filter cake was monitored. Within the interval of the sampling time t_{sample} specimen of the filter cake were taken. Wet and dry mass were determined and the solvent content was calculated by:

$$SC = \frac{m_{\mathrm{c,wet}} - m_{\mathrm{c,dry}}}{m_{\mathrm{c,wet}}} \tag{6}$$

with the masses of the dry $m_{\mathrm{c,dry}}$ and wet filter cake $m_{\mathrm{c,wet}}$. The wet mass was measured immediately after sampling and the dry mass after two weeks of drying in a vacuum oven at a pressure of 600 mbar and a temperature of 60 °C. In both cases, a laboratory balance was used to detect the weight (Kern & Sohn GmbH, Bahlingen, Germany).

3 Results and Discussion

In this section, the results are presented and discussed. Therefore, the individual process steps are first considered independently of each other. This is followed by a comparison of the results from the lab and theoretical model with those from the pilot scale and a quantification of the potential of the plant concept.

3.1 Cooling Crystallization

The production process on the integrated plant presented starts with the cooling crystallization step. Four temperature modules were used for this purpose. The cycle time was 20 min each, resulting in a total crystallization duration of 80 min. As it has been demonstrated in [5], [15], and [18] for lab-scale plants with the same operation principle, the crystallization on the respecting pilot plant showed similar results regarding growth rates, product crystal size, and yield.

The development of the PSD over time can be seen in Fig. 4. Black represents the distribution of particles in the initial feed. Gray, green, violet, and red indicate the size characteristics after several process times between 20 and 80 min. All distributions were derived from the raw data of the triple experiments via a method of smallest error.

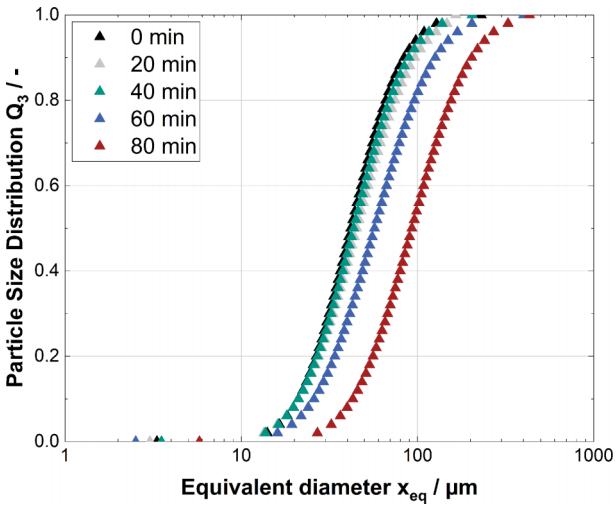

Figure 4. Temporal time evolution of the particle size distribution during the crystallization process.

The data suggests that the seed crystals were growing along the crystallization process. Starting at a median diameter of 41.86 ± 3.45 µm, the particles increase to an $x_{50,3}$ of 101.88 ± 5.41 µm as the final crystallization time of 80 min was reached. The distributions seemed to be parallel and shift from smaller to bigger crystals over the process time. That fact is also underlined by the span calculated as:

$$\text{span} = \frac{x_{90,3} - x_{10,3}}{x_{50,3}} \quad (7)$$

which shows slight deviations but not a major increase from 1.52 to 1.69 (see Tab. 2).

Table 2. Average crystal size $x_{50,3}$ and span.

Process time [min]	$x_{50,3}$ [µm]	Span [–]
0	41.86 ± 3.45	1.52 ± 0.35
20	49.81 ± 3.12	1.70 ± 0.32
40	48.39 ± 2.16	1.55 ± 0.31
60	64.07 ± 1.76	1.45 ± 0.09
80	101.88 ± 5.41	1.69 ± 0.40

Referring to the development of the median diameter in Fig. 5, the growth rate was moderate in the first 40 min and reached its maximum between 60 and 80 min. We conclude that this behavior was caused by slow transport phenomena due to the high viscosity of the system. This in turn led to strong supersaturation and higher growth rates as the process time progressed.

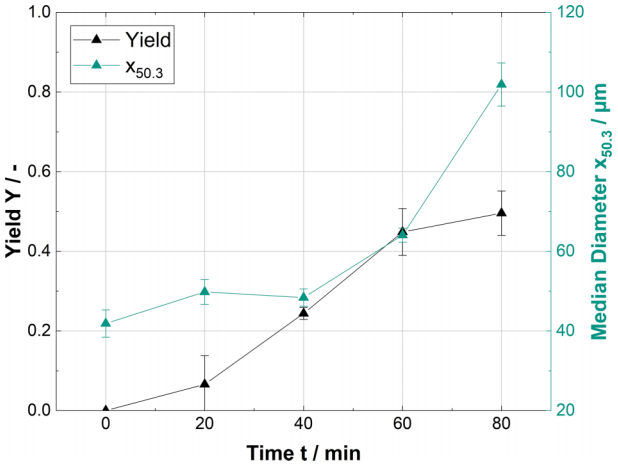

Figure 5. Time course of yield and median diameter. Both values increase with time, which indicates successful crystallization.

Just as the crystal size increased, also the relative yield rose over time (see Fig. 5). The final yield after 80 minutes of crystallization came out to be 50.0 %. The deviation from a maximum yield of 100 % indicates that the system either exhibited a higher final temperature than anticipated or that it failed to reduce the existing supersaturation by crystal growth. A combination of both is also possible.

3.2 Solid-Liquid Separation

After the cooling crystallization process, the product suspension was filtered for 20 min at a pressure difference of 500 mbar to remove the mother liquor from the slurry. For this purpose, the process medium was transferred to a filtration unit with a connection for a vacuum pump, as described in Sect. 2.1. After the cooling crystallization process, which lasted 80 min, the solvent content $SC_{80\text{min}}$ was 0.29 (see Tab. 3).

Table 3. Solvent content, $x_{50,3}$, and span during the process.

Process time [min]	SC [–]	$x_{50,3}$ [µm]	Span [–]
0	–	41.86 ± 3.45	1.52 ± 0.35
80	0.29 ± 0.00	101.88 ± 5.41	1.69 ± 0.40
100	0.09 ± 0.01	98.68 ± 3.66	1.85 ± 0.08

The filtration process decreased the solvent content to 0.09 ± 0.01, suggesting that the filtration step results in a relatively dry filter cake, which can subsequently be easily removed from the filter by a scraper. Such a removal process is pictured in Fig. 6.

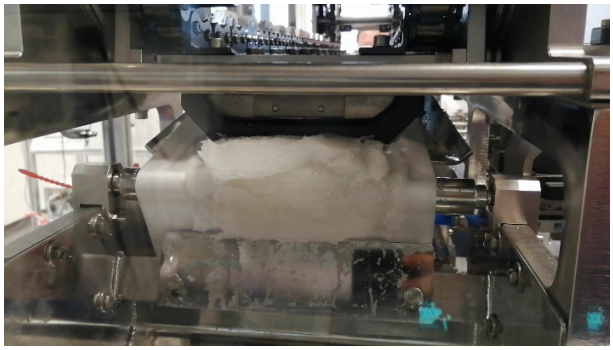

Figure 6. Removal of a dewatered cake from the pilot plant. For this, a scraper was used.

In addition to the solvent content in the cake, the influence of the filtration process on the size properties of the resulting crystals was investigated. The obtained sum distribution is presented in Fig. 7. Black indicates the seed crystals, while gray represents the state after crystallization and green that after solid-liquid separation. The diagram illustrates that the curves are nearly congruent for crystallization and filtration. The median diameters were 101.88 ± 5.41 µm after crystallization and 98.68 ± 3.66 µm after the filtration step. The span was also in a similar size range with values of 1.69 ± 0.40 and 1.85 ± 0.08. Hence, it can be concluded that the crystal size properties of the filter cake were almost influenced solely by the experimental parameters of the cooling crystallization. The filtration process seems to have only a marginal influence on the crystal properties in terms of their size distribution.

3.3 Comparison with Lab and Modeling Results

Part of this study was not only to characterize the pilot plant and demonstrate the capabilities of the production concept but also to show, on the one hand, the transferability of laboratory experiments to the pilot scale and, on the other hand, the

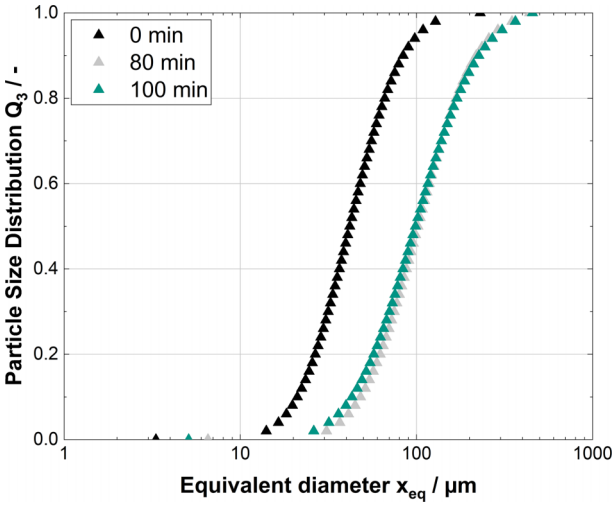

Figure 7. Crystal size distribution of seed crystals (0 min), after crystallization (80 min), and after filtration (100 min). It is found that the size properties are only marginally affected by the filtration process.

power of prediction through modeling. Regarding the transferability, experiments with the same conditions as presented before were performed on a lab-scale plant according to [15] and [18]. The dimensions of the functional units and thus the size of the detached zones varied from lab to pilot scale. With a constant filling level of 20 mm in both cases, the volumes were therefore 77.28 mL in lab scale and 240 mL in pilot scale. For the theoretical investigation, the model approach discussed in Sect. 2.3 was used. The experimental parameters from Tab. 1 were selected as input variables.

Tab. 4 presents the results from the two different plant scales and the modeling data. Comparing the experimental results, it is noticeable that the median particle sizes of the seed crystals $x_{50,3,0min}$, after crystallization $x_{50,3,80min}$, and after solid-liquid separation $x_{50,3,100min}$ were almost the same. This indicates that a size-independent scale-up was possible. Moreover, the table illustrates that the final solvent content after solid-liquid separation SC_{100min} and the yield Y_{80min} were also scale-independent process variables.

Only the distribution width and the solvent content after crystallization SC_{80min} differed between the laboratory and the pilot plant. The span in the laboratory tests was always smaller than that of the experiments carried out in the industrial environment. The explanation for this becomes apparent when looking at the surface area-to-volume ratios SA/V of the process medium. The following applies:

$$SA/V = \frac{\text{Surface Area Process Medium}}{\text{Volume Process Medium}} \tag{8}$$

While SA/V_{lab} equals 0.17 mm^{-1}, SA/V of the pilot plant is smaller with a value of 0.14 mm^{-1}. A lower SA/V causes a less homogeneous heat loss and therefore a wide and uneven temperature distribution within the suspension. This in turn creates larger variations in local supersaturations, which lead to a bandwidth of growth and nucleation rates generating product crystals with higher span. Furthermore, it can be assumed that the average temperature of the suspension for the pilot-scale experiments was higher compared to the lab-scale experiments, also caused by the ratio SA/V. This results in less crystal growth and would explain the difference in solvent content SC_{80min}.

The inputs to the modeling differ slightly from the experiments because, for modeling stability, the seed size distribution was considered based on a number-based approach rather than a volume-based approach. While the median particle diameter was predicted to be of a reasonable size compared to experiments, there were large deviations in the span and the yield, which is due to the complex processes that cannot be represented by the first-principle model. Complex modeling approaches would be necessary here, but these would greatly increase the simulation time. Nevertheless, the solvent content after solid-liquid separation SC_{100min} was close to the values actually obtained in the experiments. In sum, it can be stated that the model can provide a first good prediction of the overall process.

Table 4. Summary of the product crystal properties after crystallization and filtration for experiments and modeling.

Process step	Parameter	Lab scale	Pilot scale	Modeling results
Crystallization	$x_{50,3,0min}$ [µm]	45.03 ± 3.47	41.86 ± 3.45	39.38
	$span_{0min}$ [–]	1.16 ± 0.12	1.52 ± 0.35	0.93
	$x_{50,3,80min}$ [µm]	97.54 ± 6.00	101.88 ± 5.41	108.61
	$span_{80min}$ [–]	1.39 ± 0.10	1.69 ± 0.40	0.35
	Y_{80min} [–]	0.54 ± 0.05	0.50 ± 0.06	0.77
Solid-liquid separation	SC_{80min}	0.23 ± 0.01	0.29 ± 0.00	0.285
	SC_{100min} [–]	0.09 ± 0.01	0.09 ± 0.01	0.12
	$x_{50,3,100min}$ [µm]	99.18 ± 2.57	98.68 ± 3.66	108.61
	$span_{100min}$ [–]	1.38 ± 0.13	1.85 ± 0.08	0.35

3.4 Potentials of the Apparatus Concept

In the previous chapters, it was shown that the apparatus concept is suitable for the integrated production and separation of crystals and thus represents an alternative to already established process chains. Compared to conventional manufacturing techniques, the belt crystallizer has a number of advantages. Since the resulting market and competitive potential is strongly dependent on the material system, a qualitative evaluation including a rough estimate of these aspects is given below.

- Modular Design: According to VDI 2776 [24], the belt crystallizer is a modular plant, consisting of autonomously operating and interlinked individual components. These so-called process equipment assemblies (PEAs) can be combined as required, which significantly increases the number of degrees of freedom in process control and allows adaptation to more and more volatile markets. In addition, the versatility of the plant concept enables the realization of individual process chains and the manufacture of a wide variety of products on a single plant. The modular design ensures short changeover and retooling times (depending on the substance system and application, savings of up to 50 % may be conceivable) as well as uncomplicated replacement of defective components. Another advantage of the plant concept is the possibility of reusing the PEAs. The existing process modules (in our case, e.g., the temperature and filtration units) can be easily adapted for new plant configurations and ideas, thus considerably shortening the time-to-market along with the design and investment costs. According to initial estimates, up to 20 % of costs and energy can be saved.
- Integrated Design: The integrated design eliminates the need for typical piping and material transport equipment, which can lead to a footprint that is up to 20 % smaller and to savings of at least 10 % in investment costs. In addition, the compact design also enables significantly simplified implementation of safety guidelines – such as the realization of an inert gas atmosphere – and at the same time reduces the risk of product contamination. The latter ensures an improvement in product quality, increases production efficiency, and is thus particularly relevant for high-priced products in the specialty chemicals and pharmaceutical industries.
- Process Control: Demarcated from each other by separator plates, the individual zones pass through the process chain. This has a number of advantages, as it combines the benefits of both batch and continuous operation. On the one hand, continuous process control enables a reduction in energy-intensive startup and shutdown processes (energy savings of up to 20 % are conceivable here compared with conventional manufacturing) as well as an increase in yield up to the double-digit percentage range. On the other hand, the separation of the zones ensures that the product quality of each segment can be checked independently of one another. This allows quality fluctuations or product contamination to be detected at an early stage and affected batches to be separated from the value product. The traceability of the individual batches even makes it possible to use the system in Good Manufacturing Practices (GMP) environments.
- Automation and Process Modeling: The belt crystallizer offers a high degree of automation, as all process variables can be individually measured and controlled by a superordinate control layer. A simple model is also already available and allows the complete process chain to be computed within the framework of various assumptions in a comparatively short calculation time. By further optimizing the modeling approach and integrating suitable measurement technology (depending on the respective target variables and the material system), it is feasible to react in-situ to existing disturbances and to run the process completely autonomously in the future.
- Scalability: The plant concept is based on a conventional band filter, which is easily scalable. The experiments carried out at different dimensions indicate that the belt crystallizer seems to be a well-scalable apparatus, too. According to this it is possible to acquire a high level of process understanding even at small scales and to determine process functions in a resource-efficient manner. In addition, scalability allows production capacity to be adjusted to the existing market and product demand at any time.

4 Conclusion

To meet the existing challenges in the chemical industry, innovative solutions are required. For this reason, a modular and integrated plant concept for the quasi-continuous production of crystalline products was designed and characterized in a university environment using the model system sucrose-water. Based on the promising results, a scale-up to pilot size and a first commissioning in an industrial environment was realized. In the course of the conducted experiments, it was possible to produce a dried product filter cake from an initially added seed suspension. In addition, transferability from laboratory to pilot scale has been demonstrated. Finally, a comparison between computer model and experiment showed that the overall process can be described relatively efficiently using a simple mathematical approach.

In summary, the plant discussed can be applied in the production of fine and specialty chemicals whenever a flexible apparatus with fast retooling times is required. As an integrated concept in the downstream part of the production, it overcomes classic challenges of continuous crystallization such as blockages and clogged pipelines as well as the isolation of solid products.

Acknowledgment

The authors would like to thank the German Federal Ministry for Economic Affairs and Climate Action for financial support of this work. This research was carried out within the framework of the ENPRO initiative (funding code: 03ET1652). Furthermore, we would like to thank all participating companies for their support. In particular, we would like to thank BHS-Sonthofen GmbH for designing and manufacturing the pilot plant, SONOTEC GmbH for providing the ultrasonic sensors, HiTec Zang GmbH for the automation, and Clariant Produkte (Deutschland) GmbH for contributing the laboratory infrastructure. Open access funding enabled and organized by Projekt DEAL.

The authors have declared no conflict of interest.

Appendix

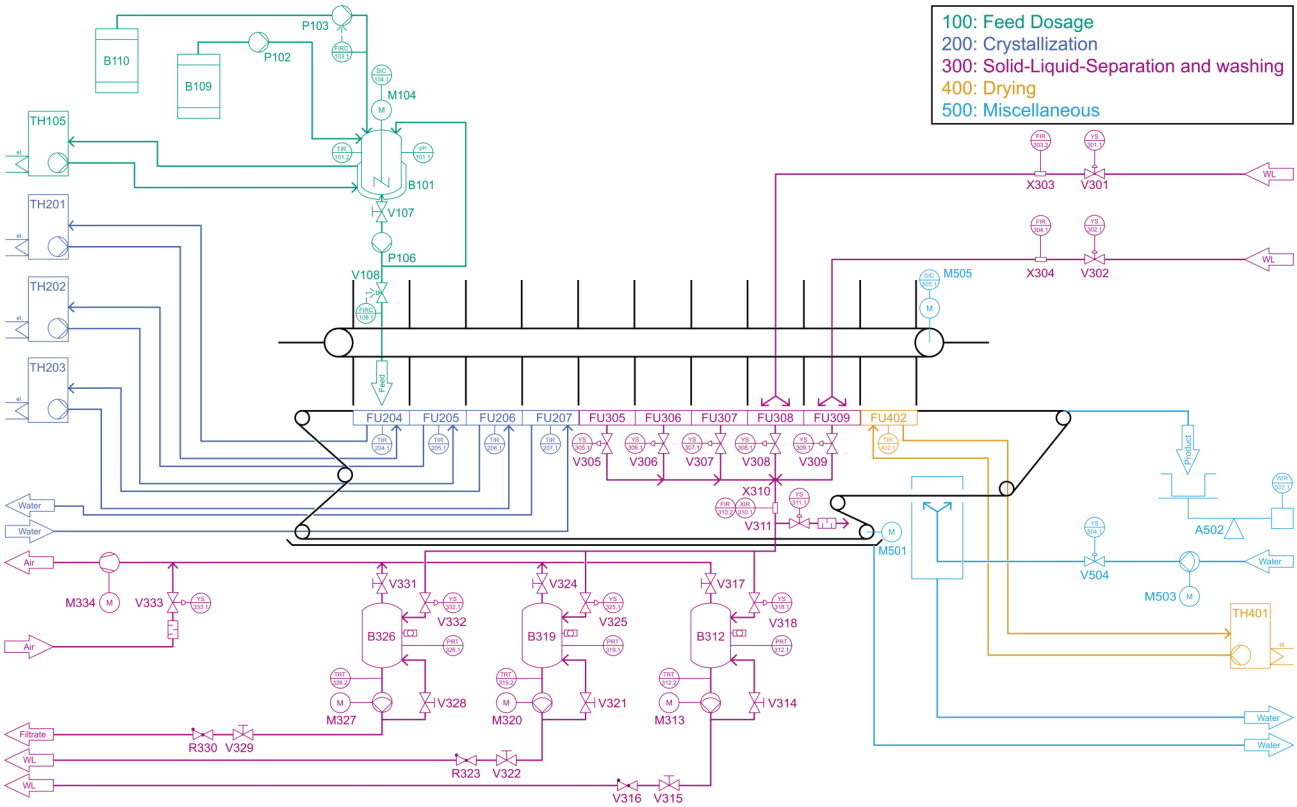

Figure A1. Piping and instrumentation diagram of the pilot plant.

Symbols used

h	[m]	height
m	[kg]	mass
n	[–]	amount
p	[kg m^{-1}s^{-2}]	pressure
SC	[–]	solvent content
t	[s]	time
T	[K]	temperature
V	[m^3]	volume
w	[–]	solid mass fraction
x	[–]	mass content
X	[–]	loading
Y	[–]	yield

Sub- and superscripts

*	saturated state
aq	aqueous
c	cake
eq	equivalent
filt	filtration
lab	laboratory
min	minutes
ml	mother liquor
mod	modules
sat	saturated
suc	sucrose
susp	suspension
theo	theoretical
tot	total

Abbreviations

ECM	excess crystal mass
PSD	particle size distribution

References

[1] T. Bieringer, S. Buchholz, N. Kockmann, *Chem. Eng. Technol.* **2013**, *36 (6)*, 900–910. DOI: https://doi.org/10.1002/ceat.201200631

[2] A. Reitze, N. Jürgensmeyer, S. Lier, M. Kohnke, J. Riese, M. Grünewald, *Angew. Chem., Int. Ed.* **2018**, *130 (16)*, 4318–4324. DOI: https://doi.org/10.1002/ange.201711571

[3] T. Seifert, S. Sievers, C. Bramsiepe, G. Schembecker, *Chem. Eng. Process.* **2012**, *52*, 140–150. DOI: https://doi.org/10.1016/j.cep.2011.10.007

[4] A. Behr, V. A. Brehme, C. Ewers, H. Grön, T. Kimmel, S. Küppers, I. Symietz, *Chem. Ing. Tech.* **2003**, *75 (4)*, 417–427. DOI: https://doi.org/10.1002/cite.200390084

[5] L. Löbnitz, Auslegung des Separationsprozesses und Entwicklung neuer Verfahrenskonzepte zur integrierten Produktion und Separation kristalliner Aminosäuren, *Ph.D. Thesis*, Karlsruher Institut für Technologie **2020**.
[6] T. Wang, H. Lu, J. Wang, Y. Xiao, Y. Zhou, Y. Bao, H. Hao, *J. Ind. Eng. Chem.* **2017**, *54*, 14–29. DOI: https://doi.org/10.1016/j.jiec.2017.06.009
[7] D. Zhang, S. Xu, S. Du, J. Wang, J. Gong, *Engineering* **2017**, *3 (3)*, 354–364. DOI: https://doi.org/10.1016/J.ENG.2017.03.023
[8] B. Wood, K. P. Girard, C. S. Polster, D. M. Croker, *Org. Process Res. Dev.* **2019**, *23 (2)*, 122–144. DOI: https://doi.org/10.1021/acs.oprd.8b00319
[9] J. Orehek, D. Teslić, B. Likozar, *Org. Process Res. Dev.* **2021**, *25 (1)*, 16–42. DOI: https://doi.org/10.1021/acs.oprd.0c00398
[10] A. Cote, D. Erdemir, K. P. Girard, D. A. Green, M. A. Lovette, E. Sirota, N. K. Nere, *Cryst. Growth Des.* **2020**, *20 (12)*, 7568–7581. DOI: https://doi.org/10.1021/acs.cgd.0c00847
[11] M. Baldea, T. F. Edgar, B. L. Stanley, A. A. Kiss, *AIChE J.* **2017**, *63 (10)*, 4262–4272. DOI: https://doi.org/10.1002/aic.15872
[12] L. Hohmann, L. Löbnitz, C. Menke, B. Santhirakumaran, P. Stier, F. Stenger, F. Dufour, G. Wiese, S. zur Horst-Meyer, B. Kusserow, W. Zang, H. Nirschl, N. Kockmann, *Chem. Eng. Technol.* **2018**, *41 (6)*, 1152–1164. DOI: https://doi.org/10.1002/ceat.201700657
[13] C. Steenweg, A. I. Seifert, N. Böttger, K. Wohlgemuth, *Org. Process Res. Dev.* **2021**, *25 (11)*, 2525–2536. DOI: https://doi.org/10.1021/acs.oprd.1c00294
[14] C. Steenweg, A. I. Seifert, G. Schembecker, K. Wohlgemuth, *Org. Process Res. Dev.* **2021**, *25 (4)*, 926–940. DOI: https://doi.org/10.1021/acs.oprd.0c00550
[15] T. Dobler, S. Buchheiser, M. Gleiß, H. Nirschl, *Processes* **2021**, *9 (4)*, 663. DOI: https://doi.org/10.3390/pr9040663
[16] F. Thurner, *Chem. Ing. Tech.* **1990**, *62 (9)*, 753–755. DOI: https://doi.org/10.1002/cite.330620914
[17] T. Dobler, B. Radel, M. Gleiss, H. Nirschl, *Crystals* **2021**, *11 (6)*, 713. DOI: https://doi.org/10.3390/cryst11060713
[18] S. Höving, B. Oldach, N. Kockmann, *Processes* **2022**, *10 (6)*, 1047. DOI: https://doi.org/10.3390/pr10061047
[19] J. Sonnenschein, M. Hermes, S. Höving, N. Kockmann, K. Wohlgemuth, *Comput. Chem. Eng.* **2022**, *167*, 108024. DOI: https://doi.org/10.1016/j.compchemeng.2022.108024
[20] A. J. C. Wilson, *Acta Crystallogr.* **1966**, *20 (1)*, 152. DOI: https://doi.org/10.1107/S0365110X66004535
[21] H. Anlauf, *Wet Cake Filtration: Fundamentals, Equipment, Strategies*, Wiley-VCH, Weinheim **2020**.
[22] E. Tsotsas, in *Handbuch Vakuumtechnik* (Ed: K. Jousten), Springer Reference Technik, Wiesbaden **2017**.
[23] T. Detloff, T. Sobisch, D. Lerche, *Part. Part. Syst. Charact.* **2006**, *23 (2)*, 184–187. DOI: https://doi.org/10.1002/ppsc.200601028
[24] VDI 2776, *Process Engineering Plants – Modular Plants – Fundamentals and Planning Modular Plants*, VDI guideline, Verein Deutscher Ingenieure, Düsseldorf **2020**.

